



Original Research Paper

## Lime-assisted hydrothermal humification and carbonization of sugar beet pulp: Unveiling the yield, quality, and phytotoxicity of products

Mona Ghaslani<sup>1</sup>, Reza Rezaee<sup>1</sup>, Omid Aboubakri<sup>1</sup>, Ehsan Sarlaki<sup>2</sup>, Thomas Hoffmann<sup>3</sup>, Afshin Maleki<sup>1,\*</sup>, Nader Marzban<sup>3,\*</sup>

<sup>1</sup>Environmental Health Research Center, Research Institute for Health Development, Kurdistan University of Medical Sciences, Sanandaj, Iran.

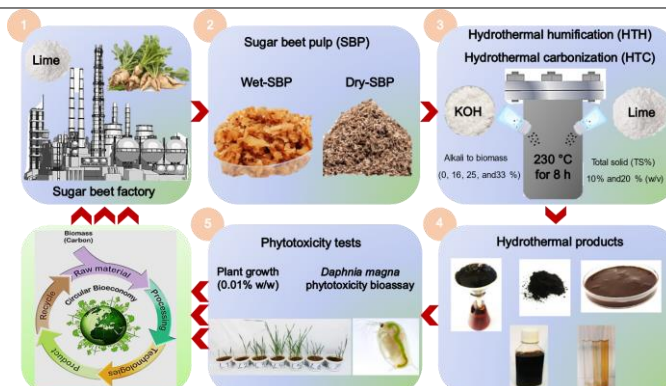
<sup>2</sup>Department of Agrotechnology, Faculty of Agricultural Technology, University of Tehran, Pakdasht, Tehran, Iran.

<sup>3</sup>Leibniz Institute for Agricultural Engineering and Bio-economy e.V. (ATB), Max-Eyth-Allee 100, 14469 Potsdam, Germany.

### HIGHLIGHTS

- Lime can be considered a cost-effective alternative to KOH in hydrothermal humification.
- Lime could significantly reduce aromatics while increasing sugars and acids.
- Wet biomass outperformed dry biomass in the process, reducing the need for pre-drying.
- A 0.01% addition of hydrothermal humification products notably enhanced plant growth.
- Hydrothermal liquid products showed no toxicity in *Daphnia magna* bioassays.

### GRAPHICAL ABSTRACT



### ARTICLE INFO

#### Article history:

Received 20 January 2024

Received in revised form 23 February 2024

Accepted 24 February 2024

Available online 1 March 2024

#### Keywords:

Sugar beet pulp  
Hydrothermal humification  
Hydrothermal carbonization  
Artificial humic acids  
Hydrated lime  
Phytotoxicity

### ABSTRACT

Hydrothermal carbonization (HTC) solid and liquid products may inhibit seed germination, necessitating post-treatment. The hydrothermal humification (HTH) method addresses this drawback by transforming inhibitory compounds, such as aromatics, into artificial humic acids (AHAs) and artificial fulvic acids (AFAs). This study introduces a novel approach by investigating the substitution of the commonly used alkaline agent in HTH, KOH, with hydrated lime to develop cost-effective hydrothermal fertilizers from sugar beet pulp, enriching them with AHAs. It assesses the effects of lime on AHA production and soluble organic compounds compared to KOH. The results indicate that lime significantly reduces furans (from 560 to 3.15 mg/kg DM in solid and from 344 to 3.86 mg/L in process liquid) and boosts sugars and organic acids, especially lactic acid (from 4.70 to 65.82 g/kg DM in solid and from 4.05 to 22.89 mg/L in process liquid), increasing hydrochar yield (68.8% with lime vs. 27.4% with KOH). Despite the lower AHA production with lime compared to KOH (3.47% vs. 15.50%), lime-treated hydrothermal products are abundant in calcium and magnesium, boasting a pH of 7. This property presents a safer and more efficient alternative to hydrothermal fertilizers. The characterization of AHAs aligns with standard and natural humic substances, while lime-assisted HTH products, applied at a level of 0.01% w/w, could significantly enhance wheat growth and nutrient uptake compared to the control group. Importantly, these products show no toxicity on *Daphnia magna*, underscoring their potential for sustainable agriculture.

©2024 Alpha Creation Enterprise CC BY 4.0

\* Corresponding authors at:

E-mail address: [maleki43@yahoo.com](mailto:maleki43@yahoo.com) (Afshin Maleki); [nmarzban@atb-potsdam.de](mailto:nmarzban@atb-potsdam.de) (Nader Marzban)

Please cite this article as: Ghaslani M., Rezaee R., Aboubakri O., Sarlaki E., Hoffmann T., Maleki A., Marzban N. Lime-assisted hydrothermal humification and carbonization of sugar beet pulp: Unveiling the yield, quality, and phytotoxicity of products. *Biofuel Research Journal* 41(2024) 2025-2039. DOI: 10.18331/BRJ2024.11.1.4.

## Contents

1. Introduction.....	2026
2. Material and Methods.....	2027
2.1. Raw materials and chemical preparation.....	2027
2.2. Hydrothermal process experiments.....	2027
2.3. Artificial humic acid production.....	2027
2.4. Analytical methods.....	2028
2.5. Plant growth phytotoxicity tests.....	2028
2.6. Daphnia magna phytotoxicity bioassay test.....	2029
3. Results and Discussion.....	2030
3.1. Yield and efficiency of the hydrothermal products.....	2030
3.2. Distribution of organics in hydrothermal products.....	2031
3.3. Distribution of nutrients in hydrothermal products.....	2033
3.4. Characterization of hydrochar and artificial humic acids.....	2033
3.5. Plant growth phytotoxicity tests.....	2034
3.6. Daphnia magna phytotoxicity bioassay test.....	2036
4. Conclusions and Prospects.....	2037
Acknowledgments.....	2037
References.....	2037

## Abbreviations

ADL	Acid detergent lignin	LC50	Lethal concentration 50
ADF	Acid detergent fiber	NDF	Neutral detergent fiber
AFAs	Artificial fulvic acids	oTS	organic Total Solid
AHAs	Artificial humic acids	PL	Process liquid
ATR-FT-IR	Attenuated total reflectance-Fourier transform infrared	SEM-EDX	Scanning electron microscopy-energy dispersive X-ray
DB	Dry biomass	SBP	Sugar beet pulp
DM	Dry matter	TC	Total carbon
GI	Germination index	TGA	Thermogravimetric analysis
HAs	Humic acids	TOC	Total organic carbon
HMF	Hydroxymethylfurfural	TS	Total solids
HPLC	High-performance liquid chromatography	TS10-HTC	Biomass content 10%, no alkali
Hs	Humic substances	TS10- K33	Biomass content 10%, KOH content 33% of dry mass of biomass
HTC	Hydrothermal carbonization	TS10-L25	Biomass content 10%, Lime content 25% of dry mass of biomass
HTF	Hydrothermal fulvic acid	TS10-L33	Biomass content 10%, Lime content 33% of dry mass of biomass
HHV	Higher heating value	TS20-L25	Biomass content 20%, Lime content 25% of dry mass of biomass
HTH	Hydrothermal humification	WB	Wet biomass
ICP-OES	Inductively coupled plasma optical emission spectroscopy	UV-Vis	Ultraviolet-visible
IHSS	International Humic Substances Society		

## 1. Introduction

Meeting the challenge of producing high-quality food for 8.9 billion people by 2050 (totaling 1.5 billion tonnes) poses increasing difficulties. Consequently, there is a growing reliance on chemical fertilizers, which now account for over 70% of agricultural and food production (Rodríguez-Espinosa et al., 2023). The main drawbacks of chemical nitrogenous fertilizers include low nitrogen use efficiency by plants (less than 30%), high emissions of greenhouse gases, high production costs, and negative impacts on soil organic matter content, microbial population, and diversity (Sarlaki et al., 2023b). Farmers are ramping up their agricultural activities and relying heavily on chemical fertilizers to boost their income from farming without considering the negative impact on the environment. This issue poses a significant risk of soil degradation and a decline in organic carbon and nutrient content (Sarlaki et al., 2023a; Wei et al., 2022), potentially leading to increased soil erosion, elevated greenhouse gas emissions, nitrate contamination of groundwater, and adverse effects on soil structure, fertility, biodiversity, and biological composition. Ultimately, these consequences can result in lower-quality agricultural and food products (Yang et al., 2023).

Soil organic carbon content can be managed by adding engineered carbon-based fertilizers, such as artificial humic products and charred carbonaceous products (pyrochar and hydrochar) (Yang et al., 2021).

According to the Food and Agriculture Organization (FAO) report, sugar beet was the second most productive crop, yielding 157 million tonnes annually (García-Velásquez and Van der Meer, 2023). One of the primary by-products of the sugar beet industry is sugar beet pulp (SBP), known for its high content of nutrients, including cellulose, pectin, protein, nitrogen, and organic matter. SBP can serve as an organic amendment to enrich soil fertility (Usmani et al., 2022).

The valorization of SBP for the production of high-value-added products can enhance the circular bioeconomy of the sugar beet industry. In recent years, various thermochemical processes such as pyrolysis, gasification, hydrothermal liquefaction, hydrothermal carbonization (HTC), and hydrothermal humification (HTH) have been utilized to convert agri-food wastes into high-value products (Li et al., 2024). Hydrothermal processes, including HTC, HTH, and most recently hydrothermal fulvic acidification (HTF), offer specific advantages over other thermochemical approaches as they eliminate the need for drying of raw materials and can convert all components of the feedstock into liquid, solid, and gas products (Kohzadi et al., 2023; Sarlaki et al., 2024). Additionally, hydrothermal conversion can dissolve organic matter in the process liquid (PL), minimizing carbon dioxide emissions and contributing to environmental preservation (Wang et al., 2024).

In HTH, various factors such as the decomposition of biomass components, the transfer of nutrients (nitrogen, phosphorus, and potassium),

and heavy metals, alongside properties of the hydrothermal liquid (chemical, spectral, and phytotoxicity aspects), as well as the pore structure, surface morphology, and specific surface area of hydrochar, are greatly influenced by operational parameters like process temperature and reaction time. Additionally, factors such as reaction chemistry (solution pH) and solid loading in the reactor play significant roles (Shao et al., 2023b).

In hydrothermal processes, inorganic minerals, such as KOH, NaOH, and  $\text{NH}_4\text{OH}$ , are commonly used as alkaline catalysts (Wang et al., 2022; Zhi et al., 2022; Efremenko et al., 2023). High alkaline concentrations are needed for the hydrolysis of lignocellulosic structure, resulting in auto-neutralization by organic acids produced in the reaction and conversion of intermediate reaction products to artificial humic acids (AHAs) (Tkachenko et al., 2023). For example, researchers utilized 25 and 23 wt% of KOH to produce 7.72 g/L and 8–12% of AHAs from vegetable waste and corn stalks, respectively, at reaction temperatures of 220 and 200°C (Cao et al., 2023; Peng et al., 2023). Additionally, high alkaline consumption has been reported for other organic wastes such as vinegar fermentation waste (0.6 mol/L of KOH at 210°C for 13 h) (Jiao et al., 2023), wastewater sludge (20% KOH, 170°C for 12 h) (Cai et al., 2023), corn straw acid hydrolysis residue (1.5 mol/L KOH at 180°C for 4 h) (Deng et al., 2023), and rice straw (KOH concentration of 1.5 mol/L) (Wang et al., 2023).

In addition to increasing process costs, higher alkaline dosage alters the pH of the final product and the surface chemistry of AHAs and hydrochar, and more importantly, it creates a boundary between HTH and HTF processes (Kohzadi et al., 2023; Tkachenko et al., 2023). One of the hot topics in hydrothermal processes is the chemical properties and toxicity of hydrothermal products (AHAs and hydrochar) to aromatics (such as furans and phenols), organic acids, heavy metals, persistent free radicals, dioxins, perfluorinated chemicals, and polycyclic aromatic hydrocarbons (Marzban et al., 2023; Petrovič et al., 2023). These compounds have negative effects on seed germination and plant growth (Bona et al., 2023; Lin et al., 2024). Aromatic compounds like phenols and furans are present in HTC-derived hydrochar, and PL may restrict their direct agricultural use (Marzban et al., 2023). The phytotoxicity effects of phenolics on plants are connected to their chemical composition and concentration, which can interfere with nutrients and reduce the availability of phosphorus and nitrogen (Lin et al., 2024). HTH and, most recently, HTF were reported as promising methods that can reduce phenolic and furanic compounds in both solid and liquid products while producing macromolecules that can be classified as AHAs and artificial fulvic acids (AFAs), respectively (Tkachenko et al., 2023).

Selecting an effective and alternative alkaline catalyst for KOH in HTH processes can reduce process costs and the phytotoxicity of hydrothermal products, especially when the selected catalyst can improve the circular bioeconomy in agricultural product conversion industries. For example, lime ( $\text{Ca}(\text{OH})_2$ ), as a calcium-containing mineral, can be an effective substitute for KOH in alkaline pH regulation. Lime is utilized in the sugar beet industry to purify and protect sucrose from breaking down into glucose and fructose and to prevent the sugar syrup from becoming acidic nature (Muir, 2022). It can also serve as a valuable source of calcium oxide (CaO) for the decomposition of organic matter in SBP, hydrolysis of C-H bonds to boost the generation of humic precursors for developing synthetic humic products, and producing hydrochar for efficient soil enrichment to enhance the growth of different agricultural products, improve soil conditioning, and stabilize soil organic carbon using polyvalent cations (Chen et al., 2021; Xu et al., 2021). The use of lime for the humification of various waste materials through the composting method has been found to prevent the acidification of compost mass, reduce the proliferation of anaerobic microbes and greenhouse gas emissions, immobilize toxic heavy metals, and increase the temperature of the compost mass during composting. Overall, it has been utilized to improve the humification process (Chen et al., 2021; Xu et al., 2021; Qi et al., 2022).

To the best of our knowledge, there have been no previous studies specifically evaluating the use of lime in the HTH process, and its impact on the yield and characteristics of hydrothermal products remains unclear. Given this lack of information, the current study aimed to explore the hydrothermal conversion of SBP in order to improve the yield, quality, and phytotoxicity of products. Initially, HTC and HTH experiments were conducted under varied operational parameters, including adjustments to the total solid content of the process, as well as the type and concentration of

the alkaline catalysts (KOH and lime) utilized. Following the experiments, the properties of hydrochar, PL, and AHAs were thoroughly assessed using diverse analytical methods. In addition, the optimal hydrothermal products were subjected to wheat seed germination. This research offers new perspectives on assessing artificial and natural-sourced humic acids (HAs) and their influence on crop growth, addressing a previous gap in the literature. However, there remain unanswered questions regarding potential secondary solubilization issues and associated health risks. Therefore, this study assessed the toxicity of hydrochar soluble products and PL on *Daphnia magna* organisms.

## 2. Material and Methods

### 2.1. Raw materials and chemical preparation

The raw materials selected for this study consisted of both dry-SBP (DB) and wet-SBP (WB), which were purchased from the Hegmatan Sugar Factory in the Hamadan Province of Iran. The DB samples were grounded and sieved with a 0.5 mm mesh sieve, then stored at -20 °C to minimize microbial growth and decomposition for further experiments. To carry out the germination test, a soil sample was collected from the campus of Kurdistan University of Medical Sciences. Chemical reagents, including potassium hydroxide, calcium carbonate, and hydrochloric acid, were purchased from Sigma Aldrich. Furthermore, hydrated lime, also referred to as calcium hydroxide ( $\text{Ca}(\text{OH})_2$ ), was purchased from Pars Chemical for adjusting pH values. Natural-sourced HA isolated from lignite (stand for HA-standard, SIGMA-ALDRICH, technical grade, 53680-10G) was used for comparison with the AHA synthesized during the hydrothermal process.

### 2.2. Hydrothermal process experiments

Prior to the experiments, the raw materials, as shown in Figure 1, were dried in an oven at 105°C for 8 h to measure their moisture content (Li et al., 2023). Moisture content was determined to be 4% and 76% for DB and WB, respectively. Hydrothermal experiments were conducted in a 200 mL stainless steel hydrothermal reactor. To investigate the yield and chemical properties of the HTC products, the study analyzed the effects of two operating parameters. These factors included the ratio of alkali to biomass (0%, 16%, 25%, and 33%) and the total biomass content (TS%), which was maintained at 10% and 20% (w/v). Notably, the WB was introduced into the reactor in its moist state, with its measured moisture content being accounted for in the water content, and additional distilled water was added to achieve the targeted 10% and 20% TS. For all experiments, the hydrothermal reactor was filled to 60% of its total volume (Marzban et al., 2023). The HTH experiments were carried out in the presence of two alkaline agents (KOH and hydrated lime), and HTC was performed without an alkaline agent. The reactor was kept at 230°C for 8h. Once the reaction was completed, the reactor was cooled down overnight (Marzban et al., 2022). The solid product (hydrochar) and PL, which are shown in Figure 1, were separated by vacuum filtration through a 0.45 µm Whatman filter paper (Li et al., 2023). Subsequently, the weight of the separated products was recorded, and the yield of hydrochar was calculated according to Equation 1 (Afolabi et al., 2020).

$$\text{Hydrochar yield (wt\%)} = \frac{\text{Dry mass of hydrochar (g)}}{\text{Dry mass of raw material (g)}} \times 100 \quad \text{Eq. 1}$$

To prevent any potential damage to the structural and functional groups, the hydrochar was dried in an oven at 70°C until a constant weight (solid yield) and then ground into fine particles for further analysis (Shrestha et al., 2021). The remaining PL was stored at -20°C for further testing (Marzban et al., 2023).

### 2.3. Artificial humic acid production

The AHA content in the hydrothermal liquid product was extracted based on the method outlined in ISO 19822, with modifications proposed by Marzban et al. (2023). Following the method, hydrochar was initially separated from the PL (Fig. 1), then AHAs were separated from the PL by making a pH adjustment to 1 using 6 M HCl (Shao et al., 2023a). Next, the



**Fig. 1.** Raw materials used in hydrothermal experiments: wet SBP (a), dry SBP (b), powdered dry SBP (c), and hydrothermal products, including PL, hydrochar, AHA, and AFA.

obtained mixture was centrifuged at 4000 rpm for 5 min. After that, the solid residues (AHAs) were separated from yellowish brown-colored supernatant (AFAs) through the Whatman filter paper (Shao et al., 2022). Subsequently, the resultant AHAs were oven-dried at 60°C for 24 h (Marzban et al., 2023). The dry weight of AHA was noted to determine the yield of AHA based on Equation 2 (Peng et al., 2023).

$$AHA \text{ yield (wt\%)} = \frac{\text{Dry mass of AHA (g)}}{\text{Dry mass of raw material (g)}} \times 100 \quad \text{Eq. 2}$$

#### 2.4. Analytical methods

Various chemical and analytical techniques were employed to analyze the different raw materials and hydrothermal products (hydrochar samples and AHAs), including elemental analysis (CHNS), attenuated total reflectance-Fourier transform infrared (ATR-FT-IR), thermogravimetric analysis (TGA), ultra-violet visible (UV-Vis), scanning electron microscopy with energy dispersive X-ray spectroscopy (SEM-EDX), high-performance liquid chromatography (HPLC), and inductively coupled plasma optical emission spectroscopy (ICP-OES), and details can be found in our previous work (Marzban et al., 2023). The detergent fiber analysis of the raw materials was performed based on VDLUFA (2012; methods 6.5.1, 6.5.2, and 6.5.3) (VDLUFA, 2012), using the ANKOM A2000 Automated Fiber Analyzer (ANKOM Technology, Macedon NY, USA). The content of neutral detergent fiber (NDF), acid detergent fiber (ADF), and acid detergent lignin (ADL) was determined to calculate the content of hemicellulose, cellulose, and lignin by subtracting ADF from NDF to obtain hemicellulose, subtracting ADL from ADF to obtain cellulose, and considering ADL as the lignin content (Ghorbani et al., 2022; Marzban et al., 2023) and summarized in Table 1.

**Table 1.** Fiber analysis of two raw biomasses (wet and dry) used for the HTC and HTH processes.

Biomass	NDF (%)	ADF (%)	ADL (%)	Lignin (%)	Hemicellulose (%)	Cellulose (%)
Dry	34.49	18.69	3.34	3.34	15.80	15.35
Wet	16.69	7.44	0.79	0.79	9.25	6.65

The organic compounds such as sugars (glucose, sucrose, and fructose), aromatics (phenol, cresol, catechol, guaiacol, furfural, and hydroxymethylfurfural (HMF)), and organic acids (acetic, lactic, and formic) in hydrochar and PL were determined. The sugars and organic acids were measured by the Ultimate 3000 UPLC system from DIONEX (column: Eurokat H (300 mm; 8 mm, 10 μm), company KNAUER). The aromatic compounds were measured using an HPLC (ICS-3000) with the UV-detector (Dionex ICS 3000; Thermo Fisher Scientific Inc., USA). The inorganic content was measured using ICP-OES (ICAP6300 Duo, Thermo Scientific) with the autosampler (ASX-520, CETAC Technologies) (Marzban et al., 2023). For PL, the pH value, total carbon (TC), and total organic carbon (TOC) in PL were also measured using Shimadzu TOC-5050A Analyzer, Germany. The concentrations of phosphate, nitrate, nitrite, and ammonium in the PL and hydrochar samples were measured using an Ion Chromatograph (ICS 1000 from Thermo Fisher Scientific Inc., USA).

The total solids (TS%) content in hydrochar and AHA was determined by treating samples at 105°C for 24 h, and the ash content was determined by further treatment of dried samples at 550°C for 5 h, according to DIN EN 14775 (Celletti et al., 2021). The organic total solids (oTS%) were calculated as the difference between the total solids and the remaining ash content (Marzban et al., 2023). The elemental analyzer (Vario ELIII) from Elementar Analysensysteme in Hanau, Germany, was employed to measure the levels of carbon, hydrogen, nitrogen, and sulfur in hydrochar and AHA by using sulfonic acid as a reference. Before analysis, the sample was dried at 60°C before being submitted to the elemental analyzer. The oxygen content was determined using the relation of  $O\% = 100 - (C\% + H\% + S\% + N\% + \text{Ash}\%)$  (Wang et al., 2017). The higher heating value (HHV) of hydrochar (Eq. 3) was estimated using the correlation developed by Marzban et al. (2022), where C and O represent the carbon and oxygen percentages of the samples on a dry basis.

$$HHV \text{ (MJ/kg)} = 0.3853C + 44.98/O \quad \text{Eq. 3}$$

It is important to note that each analysis was conducted at least twice for every hydrochar and PL, using the appropriate equipment and method. The results are then presented as average values.

A Nicolet iS5 ATR-FT-IR (Thermo Scientific, Madison, WI, USA) was used to record the FT-IR spectra of the hydrochar and AHA. The surface morphology of solids was examined using the Phenom Pro desktop scanning electron microscope (Thermo Fisher Scientific, USA). Fluorescence analysis of AHA was carried out with a Perkin-Elmer LS55 Luminescence Spectrometer (Perkin-Elmer, Waltham, MA, USA). The TGA analysis was performed using STA 449 F5 Jupiter from Netzsch, Germany. UV-Vis Spectroscopy was conducted using the T70+ UV/VIS Spectrometer (PG Instruments Ltd.).

#### 2.5. Plant growth phytotoxicity tests

The soil sample was collected from the top layer of soil (0–20 cm) present in the garden of the Kurdistan University of Medical Sciences. Then, it was air-dried, thoroughly homogenized, and sieved through a 2 mm mesh to eliminate coarse stones and plant residues (Dos Santos et al., 2020). Thereby, it was stored in suitable containers for pot experiments. The soil was classified as a sandy loam texture. The pH value, humidity, and water-holding capacity of the soil were measured as 8.91, 10%, and 30%, respectively (Islam et al., 2021). After the production, analysis, and characterization of HTH products, the best lime-assisted HTH was chosen for studying the effect of each product on seed germination and plant growth, with the results being compared to those of KOH-assisted HTH products as a reference. The pot experiment received fertilization from six different groups of hydrothermal products (hydrochar (S), process liquid (PL), a mixture of hydrochar and PL (M), hydrochar-derived dissolved organic matter (E), natural-sourced HA, and AHA at three different concentrations (0.01%, 0.1%, and 1% w/w) (Fig. 2). These were all compared to a control group with no fertilization. These ratios were chosen based on the primary experiments and two types of alkali catalysts (hydrated lime and KOH).

The experimental units consisted of plastic pots with a diameter of 7 cm and a height of 7.5 cm with a capacity of 200 g soil. The lower layer of pots



**Fig. 2.** Phytotoxicity bioassay tests used in this study for different hydrothermal products such as hydrochar, PL, hydrochar-derived dissolved organic matter, AHA, HA, and the mixture of all HTH products.

contained a specified mass of pebbles, and then 140 g of soil was added. The resulting hydrothermal products were thoroughly homogenized with the entire soil. The wheat seeds underwent disinfection with alcohol for 30 s, followed by multiple washes with deionized water. Subsequently, they were soaked in deionized water for several hours (Wang et al., 2017; Fregolente et al., 2019). Afterward, 7 wheat seeds were planted in each pot at a depth of 1 cm and a distance of 1 cm from each other. All the pots were kept in the same conditions at an indoor temperature of  $22 \pm 2^\circ\text{C}$  (Shan et al., 2023).

The seeds were germinated when a length of 2 mm of shoot emerged from the seed. Irrigation, seed germination value, and aerial organ measurement were performed 24 h after initiation and continued every day at a specific time. Soil moisture was kept at 60% of the maximum water-holding capacity by weighting (Yin et al., 2022). The experiment was conducted over 20 d. After the completion of the experiments, the total number of germinated seeds in each pot was recorded, and the lengths of root and shoot were determined. Subsequently, the relative seed germination, relative root growth, and germination index (GI) were calculated using the following equations (Eqs. 4–6) (Lang et al., 2023).

$$\text{Relative seed germination (\%)} = \frac{\text{No. of germinated seeds in progressing}}{\text{No. of germinated seeds in control}} \times 100 \quad \text{Eq. 4}$$

$$\text{Relative root growth (\%)} = \frac{\text{Mean root length in treatment}}{\text{Mean root length in control}} \times 100 \quad \text{Eq. 5}$$

$$\text{Germination Index (\%)} = \frac{\text{Relative seed germination} \times \text{Relative root growth}}{100} \quad \text{Eq. 6}$$

Typically, GI values below 50% indicate high phytotoxicity, while values above 80% show no phytotoxicity (Islam et al., 2021). At the harvest stage, plant samples were removed from the soil and rinsed with water. The roots and stems of the samples were measured in mm using a ruler, and the fresh weight of the plants was measured with a laboratory scale accurate to 0.0001. The shoot and root were then placed in an oven at a constant temperature of  $80^\circ\text{C}$  to measure their dry weight using a laboratory scale (Melo et al., 2018).

## 2.6. *Daphnia magna* phytotoxicity bioassay test

A phytotoxicity bioassay test was performed to assess the effects of hydrochar-derived dissolved organic matter and PL on *Daphnia magna* through an acute toxicity test based on the OECD test 202 protocol (OECD, 2004). The examinations were carried out in the following manner: First, the stock solutions were prepared according to the EN 12457-2 protocol (Oleszczuk et al., 2013), in which they were diluted volumetrically in six various concentrations (1, 5, 10, 50, 100, and 200 mg/L) (Griffiths et al., 2021), as illustrated in Figure 2. Subsequently, 10 samples of *Daphnia magna* neonates, each 24 hours old, were subjected to the examination (Petrovič et al., 2023). The hydrothermal products were exposed to the test organism for a duration ranging from 12 to 96 h while maintaining a temperature of  $20 \pm 1^\circ\text{C}$ . Finally, the number of immobilized microorganisms was determined, whereas *Daphnids* that were incapable of movement for 15 s after gentle agitation were classified as either immobile or dead (Griffiths et al., 2021). The experimental organisms did not receive food during the investigation. To ensure the accuracy of the examination, control groups were conducted. To quantify the toxicity of the products, the lethal concentration 50 (LC50) was utilized, which refers to the concentration level required to decrease 50% in the population of organisms that have been exposed (24 h-LC50). The LC50 values were computed via probit analysis utilizing the SPSS software.

### 3. Results and Discussion

#### 3.1. Yield and efficiency of the hydrothermal products

Figure 3a shows the solid yield and AHA yield. In the TS content of 10% KOH-assisted hydrothermal products, the solid yield was lower compared to HTC (without alkaline treatment). However, the addition of KOH increased the solid yield, and the yield of AHA was significantly increased from 0.5% (in HTC) to 15.5% when WB was utilized. Therefore, the KOH-assisted hydrothermal products (TS10-K33) were selected as a reference for comparison with lime in the next sections. When utilizing 20% of the TS content of both WB and DB, the yield was increased compared to using a TS content of 10%. Specifically, at a TS content of 20%, DB yielded higher solid content but lower AHA yield. The hydrochar yield for HTC of WB (33.6%) was higher than when 16% lime was added (solid yield=20.1%), while these values for DB were 44.6% and 27.7%, respectively (Fig. 3). An increase in lime led to a higher solid yield, while an increase in the TS content from 10 to 20% resulted in an increased AHA yield. The highest solid yield (68.8%) was observed in TS20-L25 for WB. However, for DB as well, the solid yield (66.3%) was higher compared to other experiments. As can be seen in Figure 3 and Table 2, the hydrochar from HTC showed the lowest content of ash, and the majority of hydrochar was organic solids. The HTC resulted in a final pH of 4 for WB and 5 for DB. However, the addition of lime resulted in the accumulation and increase of inorganics in hydrochar. The TS20-L25 sample, which exhibited the highest solid yield, reached a neutral pH (pH=7), indicating its suitability for soil application. In contrast, the hydrothermal experiment with KOH resulted in pH values of 9 for WB and 8 for DB, which is consistent with typical outcomes for KOH-assisted HTH and HTF experiments (Tkachenko et al., 2023).

Table 2 presents the elemental analysis and HHV for WB and DB, including hydrochar and selected AHA. The carbon content was notably higher in TS10-HTC, reaching 63.92% with DB and 67.43% with WB. The hydrochar from HTC displayed the lowest ash content relative to their raw biomass feedstocks and hydrochar samples from alkaline-assisted hydrothermal processes. An increase in carbon content and a decrease in ash content resulted in a significant rise in the HHV of hydrochar samples (Marzban et al., 2022). An increase in carbon content and a decrease in ash content resulted in a significant rise in the HHV of hydrochar samples. This increase ranged from 18.30 in DB to 26.39 MJ/kg for hydrochar produced via HTC and from 17.95 in WB to 27.85 MJ/kg for its corresponding hydrochar.

The H/C and O/C ratios, detailed in Table 2 and illustrated in the Van-Krevelen diagram (Fig. 4), depict the transformation from biomass to hydrochar. The dehydration reaction, characteristic of the HTC process, led to hydrochar samples with high carbon content. These ratios were reduced to their lowest levels in HTC-derived hydrochar for both WB and DB. Conversely, hydrochar samples from alkaline-assisted hydrothermal processes showed an increase in these ratios, aligning with findings from previous studies (Tkachenko et al., 2023).

The hydrochar produced from lime and KOH-assisted hydrothermal processes had a lower carbon content compared to the raw biomass. This decrease in carbon content, which was also observed in hydrochar from the HTF process, is due to the fact that most of the carbon dissolves into the liquid phase as organic carbon and its associated organic compounds such as sugars, acids, aromatics, and both AHA and AFA (Kohzadi et al., 2023). It was observed that the ash content in hydrochar is decreased (TS10 samples) with an increase in lime dosage, leading to an accumulation of ash and a reduction in the HHV of hydrochar samples.

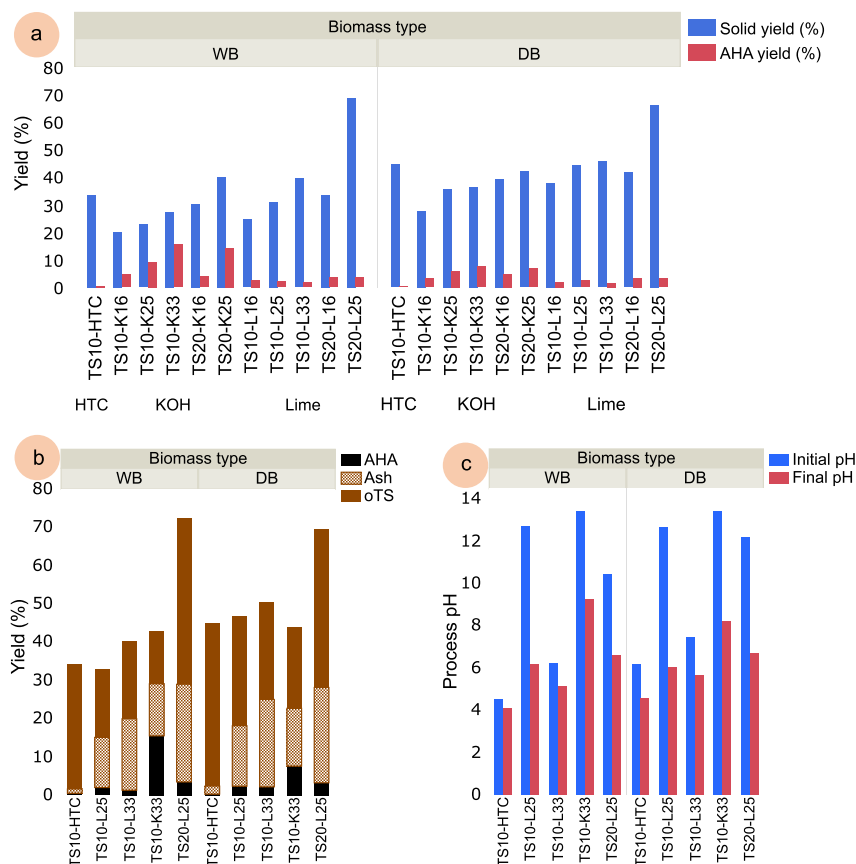
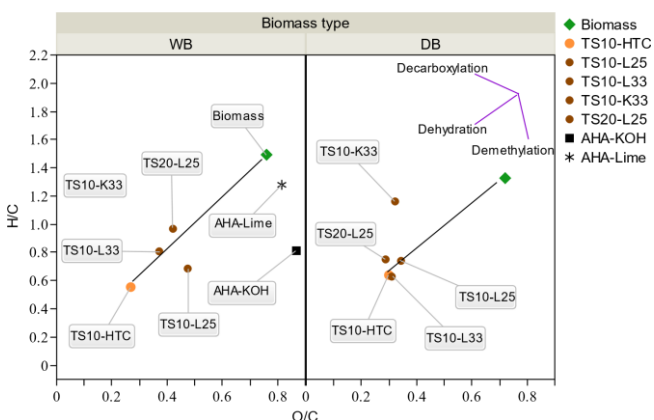


Fig. 3. Solid yield and AHA yield of the HTC process and alkaline-assisted HTH and HTF processes (a), the yield of AHA, oTS, and ash content in solid products (b), and initial and final process pH (c).

**Table 2.** Elemental analysis, O/C, and H/C ratios, as well as the HHV of biomass feedstocks, hydrochar samples, and selected AHA.

Biomass type		C (%)	H (%)	N (%)	S (%)	O (%)	Ash (%)	O/C (-)	H/C (-)	HHV (MJ/kg)
Dry	Biomass	44.77	4.96	1.69	0.12	43.00	5.46	0.72	1.33	18.30
	TS10-HTC	63.92	3.40	2.35	0.13	25.51	4.69	0.29	0.64	26.39
	TS10-L25	41.11	2.54	1.77	0.13	18.82	35.63	0.34	0.74	18.23
	TS10-L33	34.94	1.83	1.49	0.12	14.43	47.19	0.31	0.63	16.58
	TS10-K33	37.21	3.60	1.57	0.12	15.97	41.53	0.32	1.16	17.15
	TS20-L25	41.73	2.61	1.96	0.12	15.98	37.60	0.29	0.75	18.89
Wet	Biomass	43.97	5.47	1.26	0.11	44.57	4.62	0.76	1.49	17.95
	TS10-HTC	67.43	3.11	1.82	0.16	24.13	3.35	0.27	0.55	27.85
	TS10-L25	33.33	1.90	1.27	0.10	21.10	42.30	0.47	0.68	14.97
	TS10-L33	32.56	2.19	0.90	0.12	16.13	48.10	0.37	0.81	15.33
	TS10-K33	38.46	4.12	0.97	0.13	6.65	49.67	0.13	1.29	21.58
	TS20-L25	37.50	3.02	1.20	0.10	21.07	37.11	0.42	0.97	16.58
Wet	AHA-KOH	42.95	2.91	1.34	0.11	49.72	2.97	0.87	0.81	17.45
	AHA-lime	42.49	4.53	1.34	0.10	46.19	5.35	0.86	1.28	17.30



**Fig. 4.** Comparison of the molar atomic ratios of biomass feedstocks, hydrochar samples, and AHA produced via HTC and HTH (lime and KOH) of WB and DB.

The H/C ratio in alkali-assisted hydrochar was higher than those produced through HTC. While AHA-lime and AHA-KOH displayed nearly identical carbon contents, their ash content varied slightly. AHA-lime exhibited higher H/C and lower O/C ratios. Both ratios of AHAs align with those reported for artificial humic substances in previous studies (Yang et al., 2019; Dos Santos et al., 2020). Given its O/C and H/C ratios, AHA-lime closely resembles natural-sourced humic substances (HSs), as documented by the International Humic Substances Society (IHSS).

### 3.2. Distribution of organics in hydrothermal products

Figure 5 shows the content of sugars, organic acids, and aromatics in both solid and liquid products. As can be seen, fructose is a major sugar in solid and liquid products. In TS10 samples (WB), increasing lime from 0 to 25% and 33.3% led to increased fructose in both liquid and solid phases, especially in hydrochar (Fig. 5a). Sucrose and glucose levels were also increased in hydrochar with more lime, although sucrose in the liquid remained stable. Glucose in the liquid was slightly increased with a 33.3% lime addition. When the amount of WB was increased from 10% to 20%, with 25% lime, the fructose concentration in the liquid phase was increased from 11.27 to 23.97 g/L. Similarly, in the hydrochar, it was increased from 38.35 to 78.69 g/kg. Glucose and sucrose in the liquid remained constant, while in hydrochar, they were increased from 0.96 to 1.8 g/kg DM. A higher amount of sucrose was found in TS10-K33 compared to lime-treated samples (TS10-L25 and L33), while the fructose content in the solid phase was lower than that obtained from lime treatment.

In hydrothermal products of DB, with no additive (HTC), no sugars were found in the liquid, while hydrochar had a small amount of fructose (0.33 g/kg DM). Adding 25% lime led to increased glucose in both phases by 0.4 and 1 g/kg, respectively, and doubled fructose in hydrochar without affecting sucrose. Increasing lime to 33% could increase glucose levels from 0.46 to 1.37 g/kg, albeit lower than with 25% lime, where glucose was decreased to 1.14 g/kg. When TS content was increased to 20% with 25% lime, glucose in both phases was doubled. Sucrose levels remained unchanged, while fructose in hydrochar showed a slight increase (1g/kg DM).

In 10% WB, without additives, lactic and acetic acid levels in the liquid were around 4 g/L, with formic acid at 0.78 g/L (Fig. 5b). The hydrochar contained 4.69 g/kg DM of lactic acid. The addition of 25% and 33% lime significantly altered lactic acid levels in the liquid to 22.88 and 34.59 g/L, respectively, while formic acid levels in hydrochar were increased by 12 g/L and acetic acid remained constant compared to the sample with no additives. With 25% lime, total lactic acid was increased to 65.82 g/kg DM. Increasing lime to 33% showed no significant change in formic and acetic acid levels in hydrochar, at 12.94 and 15.33 g/kg DM, respectively, but lactic acid was significantly increased from 65.82 to 115.36 g/kg DM. By adding 25% lime and raising the TS content from 10% to 20%, the lactic acid concentration in the liquid was increased from 22.8 to 39.4 g/L, while the levels of formic and acetic acid were doubled. The lactic acid content in hydrochar was increased from 65 g/kg DM to over 100 g/kg DM, with formic and acetic acid also doubling in hydrochar with the increased TS content.

The same pattern for lactic acid was observed in PL of DB; however, the content of lactic acid was significantly lower compared to WB. In dry biomass with a TS content of 10% without additives (KOH or lime), acetic, formic, and lactic acid levels in the liquid were recorded at 5.16, 1.58, and 1.97 g/L, respectively, with hydrochar showing 8.05 g/kg DM of lactic acid. By incorporating 25% lime, the lactic acid concentration in the liquid was increased to 11.65 g/L, while the amount of formic acid was doubled, and there was no alteration in the level of acetic acid. The lactic acid content in hydrochar rose to 32.99 g/kg DM, but as the lime dosage was increased from 25% to 33%, the levels of formic and acetic acid in the hydrochar were decreased. However, the lactic acid content was increased to over 15 g/kg DM. When the TS content was doubled to 20% with 25% lime, the levels of lactic, formic, and acetic acid in the liquid and hydrochar were significantly increased. This finding demonstrates that the concentration of acids is increased with higher TS content and the addition of lime.

In 10% WB without additional alkaline catalyst, a notable quantity of aromatic compounds was produced (Fig. 5c). HMF was the most prominent, reaching 541.23 mg/kg DM in hydrochar and 321.94 mg/L in liquid. Catechol and phenol were also present, with catechol measuring 205.32 mg/kg DM in hydrochar and 103.97 mg/L in liquid, while phenol levels were recorded at 41.16 mg/kg DM in hydrochar. Incorporating lime at levels

ranging from 0% to 25% led to the absence of phenol. However, when the lime content was increased to 33%, the phenol level was increased to 132.00 mg/kg DM. At 25% lime, guaiacol was measured as 31.42 mg/L in liquid, and at 33% lime, it was further reduced to 19.72 mg/L, with minimal furfural formation. The addition of lime resulted in an increase in aromatic compounds in hydrochar compared to PL. When 25% lime was added, the production of guaiacol was less than 66.66 mg/kg DM. However, with 33% lime, the solid phase aromatics, such as guaiacol, phenol, and HMF, were increased by 88.78, 132.30, and 27.20 mg/kg DM, respectively. Increasing lime to 25% and TS content from 10% to 20% increased aromatics in both phases, particularly in the solid phase. No aromatic was found for TS10-K33. The TS10-L25 of WB showed significantly lower aromatics levels compared to TS10-L25 of DB.

In TS10-HTC of DB, significant levels of aromatics, including catechol, guaiacol, HMF, and furfural, were noted in the liquid phase. The total content of aromatics in DB was smaller than in WB. Adding 25% lime could significantly reduce the aromatics in the solid. Increasing lime to 33% further increased guaiacol in both phases and introduced cresol in hydrochar. When the TS content was increased from 10% to 20% with 25% lime, aromatics in the liquid phase were decreased, while they were increased in the solid phase.

Figure 5d illustrates the significant difference in TC and TOC content in the liquid phase of HTC and alkaline-assisted PL. The value of TC and TOC

of WB was higher than the corresponding conditions for processing DB. It is observed that the majority of the carbon content in the liquid is organic. Among the samples, TS20-L25 of WB exhibited the highest TC and TOC values, at 63.93 and 60.57 g/L, respectively, making the TOC content in this sample 3.62 times greater than that in TS10-HTC.

In general, using the WB as feedstock showed better performance compared to DB. For the solid phase, sugars were increased from 22.6 to 40.6 g/kg DM, with a further rise in TS content leading to 82.3 g/kg DM. Acids in the solid saw a substantial increase from 4.7 to 93.1 g/kg DM, with an enhancement in TS content resulting in 157 g/kg DM. Conversely, furans were drastically decreased from 560 to 3.15 mg/kg DM, with an increase in TS content slightly raising it to 13.8 mg/kg DM. Phenols were reduced from 246 to 66.7 mg/kg DM, with a TS content increase resulting in 172 mg/kg DM. In PL, sugars were increased slightly from 11.1 to 11.3 g/L, with an increase in TS content boosting it to 24.0 g/L. Acids were increased from 8.45 to 30.7 g/L, with an increase in TS content further elevating it to 54.1 g/L. Furans were significantly dropped from 344 to 3.86 mg/L, with an adjustment to 5.48 mg/L with an increase in TS content. Phenols were decreased from 104 to 62.8 mg/L, and an increase in TS increased it to 72.9 mg/L. Due to the higher yields of acetic acid, AHA, and solid content, as well as elevated levels of sugars and lactic acid and reduced aromatics in both solid and liquid phases, WB is a more favorable choice than DB for

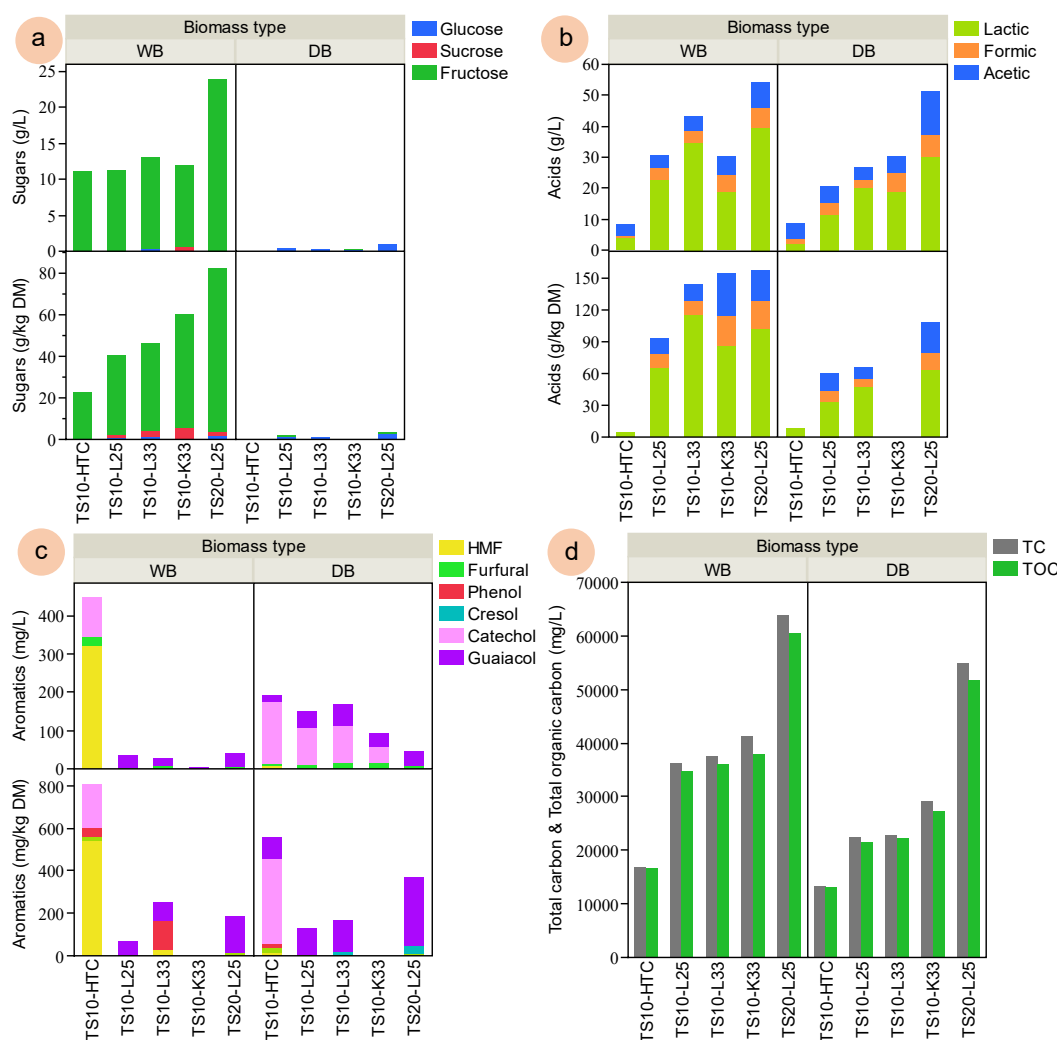


Fig. 5. Change in the concentration of a) sugars, b) organic acids, c) aromatics in the liquid (g/L) and solid (g/kg DM) products, d) TC and TOC in liquid (mg/L).

lime-assisted hydrothermal processing aimed at soil-crop application. This approach also reduces the cost associated with pre-drying SBP. The subsequent section discusses changes in inorganic elements measured by the ICP-OES method and the results of individual nitrogen and phosphorus contents.

### 3.3. Distribution of nutrients in hydrothermal products

We analyzed the distribution of inorganic compounds following hydrothermal processing. Initial observations on nutrient distribution are depicted in **Figure 6a**. Without additives (TS10-HTC), the concentration of these elements was minimal in both liquid and solid phases. In WB, an increase in lime (HT10-L25) led to a total recovery of phosphorus (P) in the solid phase at 1541 mg/kg DM, with a negligible amount (2 mg/L) detected in the liquid phase. Significantly, all solid products from the alkaline-assisted hydrothermal process exhibited higher P levels compared to HTC solids. The addition of 25% lime markedly increased levels of calcium and magnesium. The aluminum content in hydrochar was also doubled. At a concentration of 33.3% lime, the levels of calcium and magnesium were increased, while there were slight rises in manganese, aluminum, and iron.

After examining the impact of lime on WB, we looked into how changing the TS content influences the distribution of nutrients. Specifically, when the TS content of WB was increased from 10 to 20%, calcium in the liquid phase was significantly increased from 7070.25 to 12189.10 mg/L, and phosphorus increased from 1.67 to 4.98 mg/L. Magnesium, potassium, and sodium in hydrochar were also increased, while aluminum, sulfur, cobalt, cadmium, and lead were decreased. Manganese content was doubled. Conversely, in DB with lime addition, levels of phosphorus, sulfur, copper, and sodium were decreased. Increasing the TS content of DB from 10 to 20% showed no significant change in iron, calcium, and magnesium levels.

**Figure 6b** illustrates that in TS10, the total concentration of ions ( $\text{NH}_4^+$ ,  $\text{NO}_2^-$ ,  $\text{NO}_3^-$ , and  $\text{PO}_4^{3-}$ ) was increased in the liquid phase and decreased in the solid phase with the addition of lime. This pattern was similar for both WB and DB. As the TS content increased from 10% to 20%, the concentration of these compounds increased in both the solid and liquid phases, indicating a higher biomass concentration. In TS20-L25 of DB, the concentrations in both solid and liquid were higher compared to WB.

### 3.4. Characterization of hydrochar and artificial humic acids

**Figure 7a** presents the FT-IR spectra for HTC and HTH hydrochar samples alongside AHA-lime and AHA-KOH. Notable absorption bands

are observed in the of 3600–3050  $\text{cm}^{-1}$  (a wide band indicative of OH groups bonded by hydrogen), 2940–2900  $\text{cm}^{-1}$  (stretching of aliphatic C-H), 1690–1500  $\text{cm}^{-1}$  (aromatic C=C, carboxylate ions, and hydrogen-bonded carbonyl groups), 1465–1300  $\text{cm}^{-1}$  (stretching of C–O and bending of OH in carboxylic acids), and 1185–864  $\text{cm}^{-1}$  (C–O stretching in polysaccharide components). Hydrochar samples from lime and KOH-assisted HTH displayed similarities in functional groups, particularly around 1015, 1395, and 1588  $\text{cm}^{-1}$ . Comparison of commercial fulvic acid (FA) with HTH hydrochar samples revealed specific similarities at peaks 1395 and 1588  $\text{cm}^{-1}$ . The unique peaks for FA, also highlighted in **Figure 7b**, suggest that AFA, soluble across most pH ranges (Tkachenko et al., 2024), may initially form in PL of the HTH process before adsorption by the hydrochar. Hydrochar from HTC exhibited distinct peaks at approximately 1631 and 1700  $\text{cm}^{-1}$ , associated with aromatic C=C, COO-, hydrogen-bonded C=O, a structure also present in AHA-lime and AHA-KOH. Both the HA-Standard and AHAs exhibited a diverse array of peaks, which are characteristic of HSs (Aiken et al., 1986; Stevenson, 1994). Moreover, the spectra for HA and AHA indicated a decrease in absorbance with increasing wavelength (**Fig. 7b**), a feature typical of HS (Cunha et al., 2009).

**Figure 7c** shows the fluorescence and UV-Vis spectral analysis of HA-Standard, AHA-lime, and AHA-KOH. The fluorescence and UV-Vis spectral analysis indicate that AHA-lime exhibits a closer similarity to HA-Standard than AHA-KOH, as evidenced by the overlapping peaks in the fluorescence excitation-emission matrix plots in the range of 400–650 Em. (nm) and 350–500 Ex. (nm), and the comparable absorbance patterns in the UV-Vis spectra. These spectral similarities suggest that AHA-lime may have common molecular structures and functional groups, as discussed in FT-IR results, with HA-Standard. The TGA of hydrochar produced from the HTH process using lime and KOH was compared with alkali lignin as a reference (**Fig. 7d**). The results indicate that the HTH hydrochar samples display distinct degradation patterns compared to lignin, each with its unique signature. This finding suggests that the lignin present in the biomass underwent a transformation into phenols during the HTH process, as illustrated in **Figure 5**, and actively participated in the humification process rather than remaining unchanged or undergoing solely solid-solid pyrolysis reactions. This finding suggests that the selected conditions of the HTH process in this study, including the temperature and the quantities of KOH and lime used, were adequate to break down the biomass structure and promote the humification reactions.

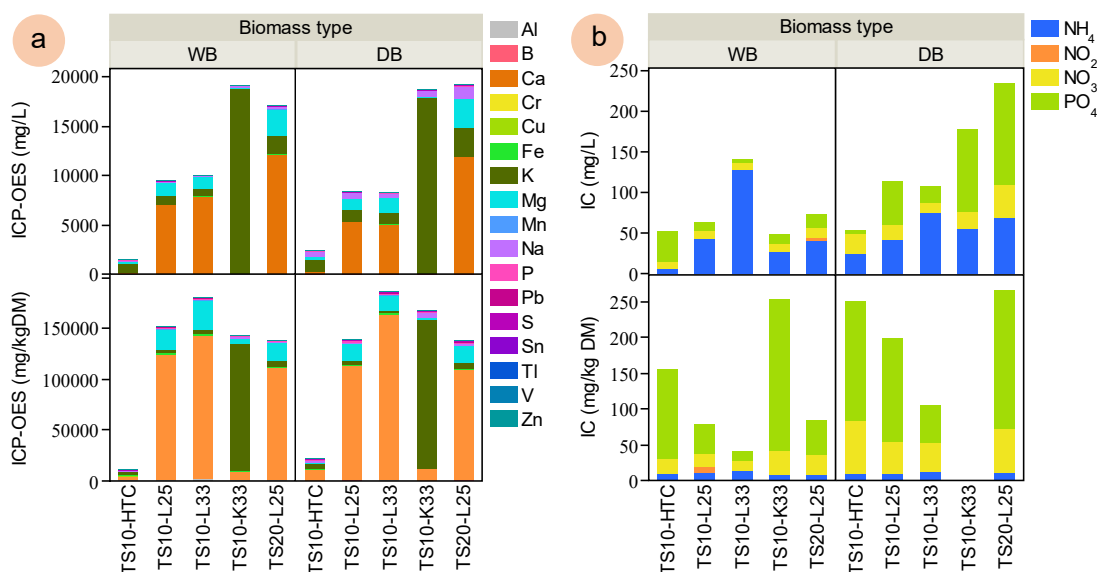


**Fig. 6.** The content of inorganics measured by the ICP-OES technique (a) and ions measured by the IC technique in the liquid (mg/L) and solid (mg/kg DM) (b).

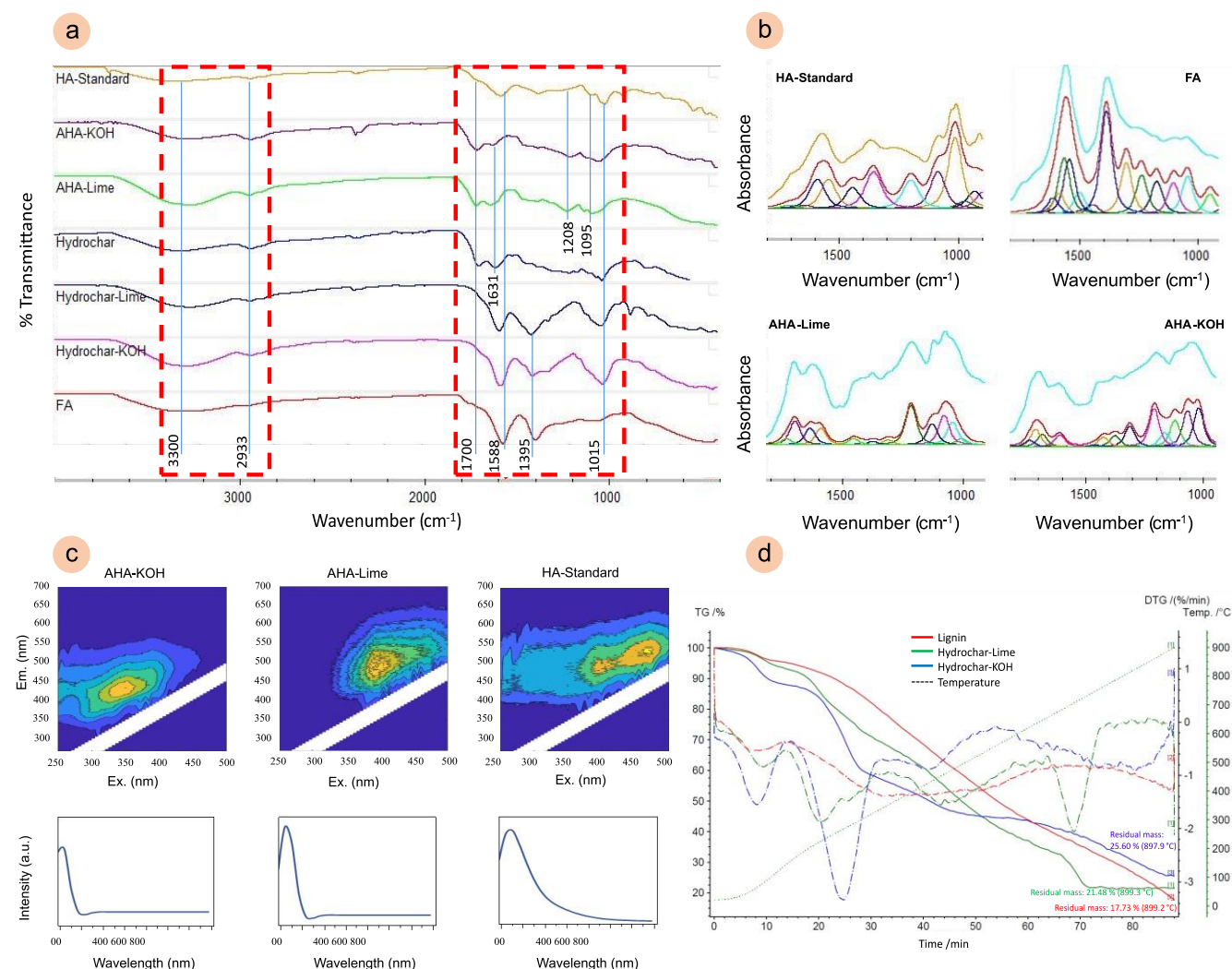


Fig. 7. FT-IR spectra of hydrochar from HTC, lime and KOH-assisted, and selected AHA (a), Absorbance of AHA, HA-Standard, and FA (b), Fluorescence and UV-vis spectra of AHA and HA-Standard (c), and comparative TGA analysis of hydrochar produced from lime and KOH-assisted hydrothermal process with alkali lignin (d).

Figure 8 displays the SEM-EDX analysis of the AHA produced with lime and KOH alongside the HA-Standard. The HA-Standard contains a significant quantity of inorganics like Na, Cl, and K, possibly from the extraction process. The Cl content in HTH-lime was 2.82 wt%, and in AHA-lime, it was 3.16 wt%, both slightly below the total ash content of AHAs presented in Table 2. The presence of Cl may occur during the precipitation and extraction phases of AHA, underscoring the importance of rinsing AHA post-extraction to eliminate contaminants. SEM images reveal the varied morphologies of hydrochar samples from HTH (Figs. 8a and b) and HTC (Fig. 8c). Lime-assisted HTH hydrochar appears smaller compared to the others. The distinctive spherical structures in HTC hydrochar (Fig. 8c) are characteristic of aromatic hydrochar samples formed from the condensation of aromatics on the surface of solid-solid reaction products, creating the spherical shape. The lack of spherical structures in HTH hydrochar indicates that the higher pH of the process reduces aromatics participating in humification reactions, leading to the creation of AHA rather than undergoing polycondensation to form secondary hydrochar.

### 3.5. Plant growth phytotoxicity tests

HTH products can enhance soil nutrients and microorganism activity, improving soil characteristics and promoting plant growth (Petrovič et al.,

2023). Figures 9a and b show the wheat GI treated with HTH products. The GI values exceeded 80%, showing no phytotoxic effects and indicating enhanced growth compared to controls due to the reduced phytotoxicity and improved root development. A minor increase of 0.01% w/w in treatment concentration significantly raised GI, attributed to humic-like substances in by-products akin to growth-promoting hormones (Fregolente et al., 2019). The results reveal that only the PL of lime-assisted HTH at a concentration of 0.01% w/w exhibited phytotoxicity, leading to a reduction in the GI. However, by increasing concentrations to 0.1% and 1% w/w, the GI was significantly enhanced.

HSS are known to plant growth hormones like indole acetic acid and gibberellins, boosting root elongation and nutrient adsorption (Yang et al., 2021). However, high concentrations of AHA can introduce phytotoxic compounds, affecting seedling and root growth (Fregolente et al., 2021). Despite not detecting catechol, phenol, or cresol, other phytotoxic elements might have influenced the results. Direct comparisons with other studies are challenging due to varying product compositions. Nevertheless, hydrothermal conversion of SBP offers a sustainable organic amendment source, crucial for soil organic matter management and recycling (Bento et al., 2021).

Here, we observed that both lime and KOH-assisted HTH products, including solid (S), liquid (L), water extract (E), mixture (M), and AHA, did

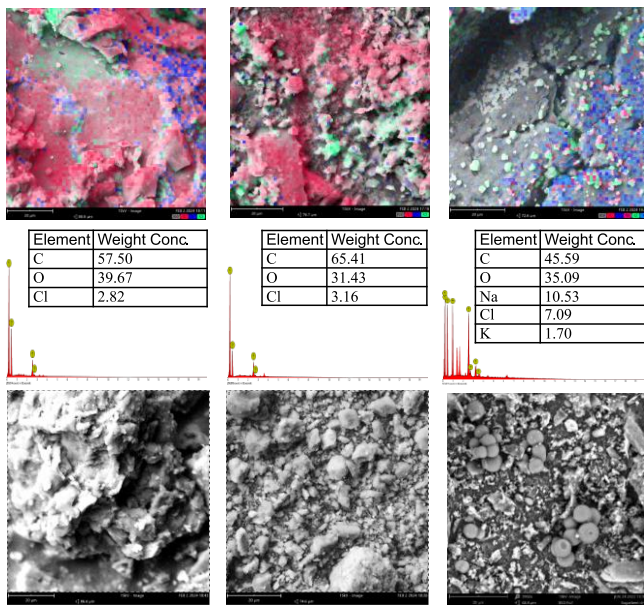


**Fig. 8.** SEM-EDX analysis of AHA-KOH (a), AHA-lime (b), HA-Standard (c), and SEM of hydrochar samples produced from KOH-assisted HTH (d), hydrochar produced from lime-assisted HTH (e), and hydrochar produced using HTC (no additive) (f).

not show phytotoxic effects. The solid product from lime-assisted HTH notably enhanced the GI compared to KOH, although the outcomes from most lime and KOH-assisted HTH products were comparable and almost identical. This finding indicates that lime could serve as an alternative to KOH in AHA production. Despite yielding less AHA, the substantial solid yield, lower corrosiveness, and its final neutral pH could compensate for the lower AHA yield. The best and most economical method to apply lime-assisted HTH products is to use them as a slurry mixture. This form of usage reduces the need for separation, extraction, and drying processes.

The plants grown in a mixture (M) from the lime- and KOH-assisted HTH processes were analyzed using elemental analysis and ICP-OES (Figs. 10a and b).

The P and K content in plants was higher in the KOH-assisted HTH mixture than in the lime-assisted HTH mixture and control. Plants grown in the KOH-HTH mixture at a 0.01% w/w level had the highest total inorganics, notably P (5814 mg/ kg DM), Fe (6988 mg/ kg DM), and Ca (9407 mg/kg DM). Increasing the KOH-HTH mixture level from 0.01% to 1% w/w reduced the inorganic content in plants. Conversely, increasing the lime-HTH mixture level from 0.1% to 1% w/w led to more inorganics absorbed by plants, which also increased stem length (Figs. 10c and d). In KOH-HTH products, stem length and plant carbon content were increased with lower inorganics (and applied level %w/w). The N content was highest (4%) in the control group and minimal (0.01%) in the mixture from the KOH-assisted HTH process. Given the higher germination GI of the lime mixture compared to KOH at 0.01% and the lower production cost, this level is recommended.

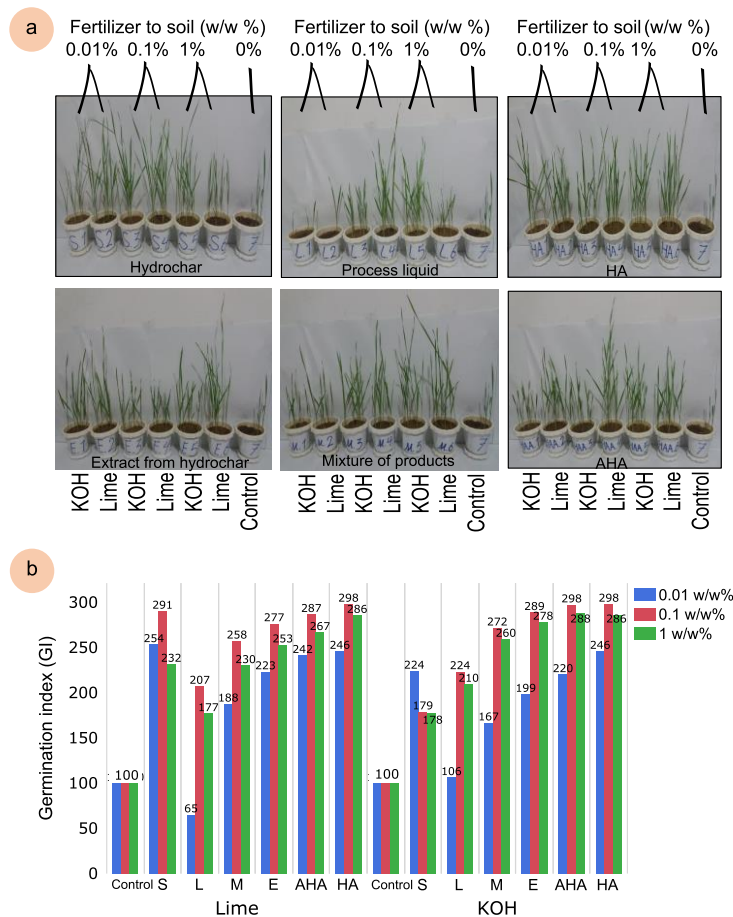


**Fig. 9.** Wheat plants (a) and GI value (b) of lime and KOH-assisted HTH products at three different applied levels to soil (w/w%).

Please cite this article as: Ghaslani M., Rezaee R., Aboubakri O., Sarlaki E., Hoffmann T., Maleki A., Marzban N. Lime-assisted hydrothermal humification and carbonization of sugar beet pulp: Unveiling the yield, quality, and phytotoxicity of products. Biofuel Research Journal 41 (2024) 2025-2039. DOI: 10.18331/BRJ2024.11.1.4.

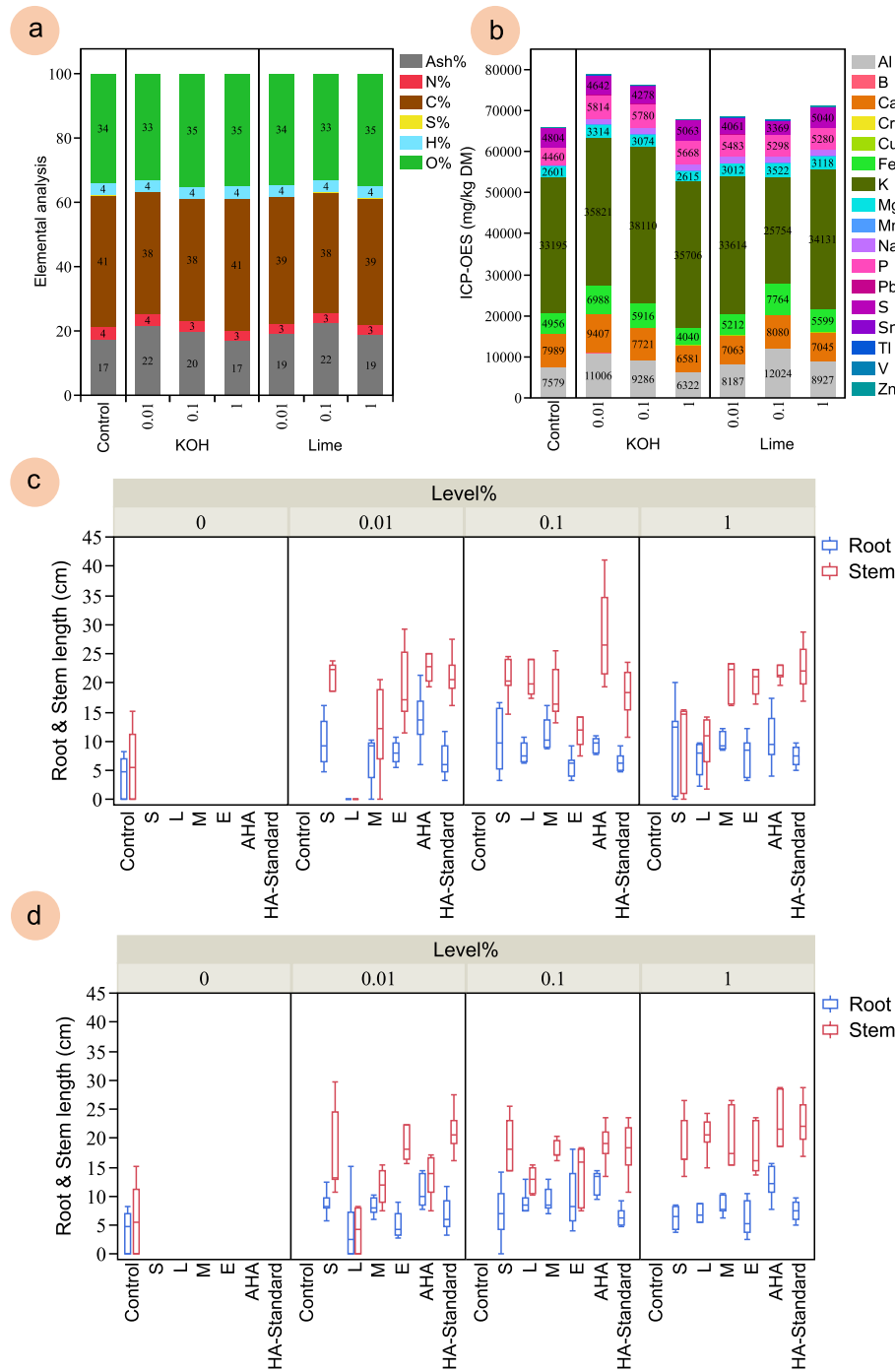


**Fig. 10.** Elemental analysis of wheat plants grown in pots treated with a mixture of HTH products (a); Inorganic content of wheat plants grown in pots treated with a mixture of HTH products (b); root and steam length of the plants grown in different applied levels of lime-assisted HTH products (c); root and steam length of the plants grown in different applied levels of KOH-assisted HTH products (d).

**3.6. *Daphnia magna* phytotoxicity bioassay test**

The results of an acute toxicity test conducted on *Daphnia magna* indicate that diluted PL did not result in the death of any *Daphnia magna* organisms. Additionally, despite the heightened sensitivity, all organisms utilized in experiments remained healthy and alive for up to 96 h, even at higher concentrations (200 mg/L). Consequently, it can be claimed that this by-product can be applied in non-toxic products without causing any

detrimental impacts on aquatic organisms. The results reported here are according to the investigation conducted by (Wang et al., 2017), which indicates that biochar samples obtained from agricultural waste are safe for soil application. In contrast, biochar derived from the *Acorus calamus* illustrates considerable toxicity in all the examined organisms at relatively high dosages. Therefore, it is imperative to conduct a risk assessment for the utilization of hydrothermal by-products before their environmental application (Wang et al., 2017).

#### 4. Conclusions and Prospects

This study examined the potential of hydrated lime as a heterogeneous alkaline catalyst compared to conventional KOH in the hydrothermal conversion of SBP valorized through the HTH and HTC processes. The study also looked at how wet and dry SBP affected the yield of AHA and hydrochar, as well as the distribution of organics and nutrients in the solid and liquid hydrothermal products. The highest solid yield and AHA were achieved when wet biomass was utilized as feedstock for the HTH process. The optimal AHA yields were found to be 15.50% with KOH and 3.49% with hydrated lime. The results also showed that the hydrochar performed optimally, with yields of 40.07% and 68.82%, respectively, for KOH and lime. The AHA produced from SBP had a stable, aromatic structure and a high degree of humification, similar to natural-sourced HAs. No significant toxic effects were also observed in the hydrothermal products. Through a direct comparison of HTC and HTH, the superior attributes of HTH become evident, yielding increased amounts of AHAs and substantially reducing aromatics. Efficient carbon flow between liquid and solid phases highlights the environmental benefits of the HTH process.

We reported that hydrated lime, used in the sugar beet industry, can effectively catalyze the hydrothermal conversion of SBP into valuable AHA and hydrochar for practical soil and agricultural applications, promoting circular economy principles within the industry. However, apart from the exciting findings in this study, there is a need for further exploration of the applications and potential of HTH processes and their products. Future research should prioritize HTH process optimization and explore the transformation and contribution of lignin, cellulose, and hemicellulose in the production of AHAs in more detail. Additionally, exploring alternative alkaline catalysts, such as other inorganic minerals like zeolite and biomass fly ash, as substitutes for KOH could enhance the sustainability and economic viability of the hydrothermal processes of biomass. The replacement of hydrated lime for KOH-catalysed HTH processes in terms of its impact on thermodynamic efficiency, techno-economic indicators, life cycle emissions, and circular bioeconomy of sugar beet conversion industries can be investigated in future studies.

#### Acknowledgments

This article was extracted from the MSc thesis of the first author. The authors would like to thank Kurdistan University of Medical Sciences and Environmental Health Research Center for the financial support provided for this research work (IR.MUK.REC.1401.394). We thank Dr. Kazem Godini for his valuable guidance and to Dr. Ali Johari for his help in conducting bioassay experiments. We thank the analytical chemistry group (Leibniz Institute of Agricultural Engineering and Bioeconomy) for their expertise and support with the analytical techniques. We also thank Giacomo Rossi, Katleen Friedrich, and Prof. Scheufele, Prof. Ribeiro for their support in performing the TGA and fluorescence and UV analysis.

#### References

- [1] Afolabi, O.O.D., Sohail, M., Cheng, Y.L., 2020. Optimisation and characterisation of hydrochar production from spent coffee grounds by hydrothermal carbonisation. *Renewable Energy*. 147, 1380-1391.
- [2] Aiken, G.R., Mcknight, D.M., Wershaw, R.L., Maccarthy, P., 1986. Humic substances in soil, sediment, and water. 1985. *Soil Sci.* 142(5), 323.
- [3] Bento, L.R., Spaccini, R., Cangemi, S., Mazzei, P., de Freitas, B.B., de Souza, A.E.O., Moreira, A.B., Ferreira, O.P., Piccolo, A., Bisinoti, M.C., 2021. Hydrochar obtained with by-products from the sugarcane industry: molecular features and effects of extracts on maize seed germination. *J. Environ. Manage.* 281, 111878.
- [4] Bona, D., Lucian, M., Ferretti, D., Silvestri, S., Zerbini, I., Merzari, F., Messineo, A., Volpe, M., 2023. Phytotoxicity and genotoxicity of agro-industrial digested sludge hydrochar: the role of heavy metals. *Sci. Total Environ.* 871, 162138.
- [5] Cai, S., Zhang, Y., Hu, A., Liu, M., Wu, H., Wang, D., Zhang, W., 2023. Dissolved organic matter transformation mechanisms and process optimization of wastewater sludge hydrothermal humification treatment for producing plant biostimulants. *Water Res.* 235, 119910.
- [6] Cao, Y., Jin, H., Zhu, N., Zhou, Z., 2023. High-efficiency fungistatic activity of vegetable waste-based humic acid related to the element composition and functional group structure. *Process Saf. Environ. Prot.* 169, 697-705.
- [7] Celletti, S., Lanz, M., Bergamo, A., Benedetti, V., Basso, D., Barattieri, M., Cesco, S., Mimmo, T., 2021. Evaluating the aqueous phase from hydrothermal carbonization of cow manure digestate as possible fertilizer solution for plant growth. *Front. Plant Sci.* 12.
- [8] Chen, Z., Fu, Q., Cao, Y., Wen, Q., Wu, Y., 2021. Effects of lime amendment on the organic substances changes, antibiotics removal, and heavy metals speciation transformation during swine manure composting. *Chemosphere.* 262, 128342.
- [9] Cunha, T.J.F., Novotny, E.H., Madari, B.E., Martin-Neto, L., de O Rezende, M.O., Canelas, L.P., de M Benites, V., 2009. Spectroscopy characterization of humic acids isolated from Amazonian dark earth soils (*Terra Preta de Índio*), in: *Amazonian Dark Earths. Wim Sombroek's Vision*. Springer. 363-372.
- [10] Deng, F., Cao, Z., Luo, Y., Wang, R., Shi, H., Li, D., 2023. Production of artificial humic acid from corn straw acid hydrolysis residue with biogas slurry impregnation for fertilizer application. *J. Environ. Manage.* 345, 118845.
- [11] Dos Santos, J.V., Fregolente, L.G., Moreira, A.B., Ferreira, O.P., Mounier, S., Viguier, B., Hajjoul, H., Bisinoti, M.C., 2020. Humic-like acids from hydrochars: study of the metal complexation properties compared with humic acids from anthropogenic soils using PARAFAC and time-resolved fluorescence. *Sci. Total Environ.* 722, 137815.
- [12] Efremenko, E., Stepanov, N., Senko, O., Lyagin, I., Maslova, O., Aslanli, A., 2023. Artificial humic substances as biomimetics of natural analogues: production, characteristics and preferences regarding their use. *Biomimetics.* 8(8), 613.
- [13] Fregolente, L.G., dos Santos, J.V., Mazzati, F.S., Miguel, T.B.A.R., de C. Miguel, E., Moreira, A.B., Ferreira, O.P., Bisinoti, M.C., 2021. Hydrochar from sugarcane industry by-products: assessment of its potential use as a soil conditioner by germination and growth of maize. *Chem. Biol. Technol. Agric.* 8, 1-13.
- [14] Fregolente, L.G., Miguel, T.B.A.R., de Castro Miguel, E., de Almeida Melo, C., Moreira, A.B., Ferreira, O.P., Bisinoti, M.C., 2019. Toxicity evaluation of process water from hydrothermal carbonization of sugarcane industry by-products. *Environ. Sci. Pollut. Res.* 26, 27579-27589.
- [15] García-Velásquez, C., Van der Meer, Y., 2023. Mind the Pulp: environmental and economic assessment of a sugar beet pulp biorefinery for biobased chemical production. *Waste Manage.* 155, 199-210.
- [16] Ghorbani, M., Li, Q., Kianmehr, M.H., Arabhosseini, A., Sarlaki, E., Asefpour Vakilian, K., Varjani, S., Wang, Y., Wei, D., Pan, J., Aghbashlo, M., Tabatabaei, M., 2022. Highly digestible nitrogen-enriched straw upgraded by ozone-urea pretreatment: digestibility metrics and energy-economic analysis. *Bioresour. Technol.* 360, 127576.
- [17] Griffiths, M.R., Strobel, B.W., Hama, J.R., Cedergreen, N., 2021. Toxicity and risk of plant-produced alkaloids to *Daphnia magna*. *Environ. Sci. Eur.* 33, 1-12.
- [18] Islam, Md Azharul, Paul, J., Akter, J., Islam, Md Atikul, Limon, S.H., 2021. Conversion of chicken feather waste via hydrothermal carbonization: process optimization and the effect of hydrochar on seed germination of *Acacia auriculiformis*. *J. Mater. Cycles. Waste Manage.* 23, 1177-1188.
- [19] Jiao, N., Zhu, Y., Li, H., Yu, Y., Xu, Y., Zhu, J., 2023. Two-Step Hydrothermal pretreatments for co-producing xylooligosaccharides and humic-like acid from vinegar residue. *Fermentation.* 9(7), 589.
- [20] Kohzadi, S., Marzban, N., Zandsalimi, Y., Godini, K., Amini, N., Puttaiah, S.H., Lee, S.M., Zandi, S., Ebrahimi, R., Maleki, A., 2023. Machine learning-based modeling of malachite green adsorption on hydrochar derived from hydrothermal fulvification of wheat straw. *Heliyon.* 9.
- [21] Lang, Q., Guo, X., Wang, C., Li, L., Li, Y., Xu, J., Zhao, X., Li, J., Liu, B., Sun, Q., 2023. Characteristics and phytotoxicity of hydrochar-

- derived dissolved organic matter: effects of feedstock type and hydrothermal temperature. *J. Environ. Sci.*
- [22] Li, C., Cai, R., Hasan, A., Lu, X., Yang, X., Zhang, Y., 2023. Fertility assessment and nutrient conversion of hydrochars derived from co-hydrothermal carbonization between livestock manure and corn cob. *J. Environ. Chem. Eng.* 11(1), 109166.
- [23] Li, X., Zhi, Y., Jia, M., Wang, X., Tao, M., Wang, Z., Xing, B., 2024. Properties and photosynthetic promotion mechanisms of artificial humic acid are feedstock-dependent. *Carbon Res.* 3, 4.
- [24] Lin, C., Xin, Z., Yuan, S., Sun, J., Dong, B., Xu, Z., 2024. Effects of production temperature on the molecular composition and seed-germination-promoting properties of sludge-based hydrochar-derived dissolved organic matter. *Water Res.* 251, 121133.
- [25] Marzban, N., Libra, J.A., Hosseini, S.H., Fischer, M.G., Rotter, V.S., 2022. Experimental evaluation and application of genetic programming to develop predictive correlations for hydrochar higher heating value and yield to optimize the energy content. *J. Environ. Chem. Eng.* 10(6), 108880.
- [26] Marzban, N., Libra, J.A., Rotter, V.S., Ro, K.S., Moloeznik Paniagua, D., Filonenko, S., 2023. Changes in selected organic and inorganic compounds in the hydrothermal carbonization process liquid while in storage. *ACS Omega.* 8(4), 4234-4243.
- [27] Melo, T.M., Bottlinger, M., Schulz, E., Leandro, W.M., de Aguiar Filho, A.M., Wang, H., Ok, Y.S., Rinklebe, J., 2018. Plant and soil responses to hydrothermally converted sewage sludge (sewchar). *Chemosphere.* 206, 338-348.
- [28] Muir, B.M., 2022. Sugar Beet Processing to Sugars, in: Misra, V., Srivastava, S., Mall, A.K. (Eds.), *Sugar Beet Cultivation, Management and Processing*. Springer Nature Singapore, Singapore. 837-862.
- [29] OECD, 2004. Test No. 202: *daphnia* sp. acute immobilisation test. OECD publishing.
- [30] Oleszczuk, P., Joško, I., Kuśmierz, M., 2013. Biochar properties regarding to contaminants content and ecotoxicological assessment. *J. Hazard. Mater.* 260, 375-382.
- [31] Peng, X., Gai, S., Cheng, K., Yang, F., 2023. Hydrothermal humification mechanism of typical agricultural waste biomass: a case study of corn straw. *Green Chem.* 25(4), 1503-1512.
- [32] Petrovič, A., Cenčič Predikaka, T., Škodič, L., Vohl, S., Čuček, L., 2023. Hydrothermal co-carbonization of sewage sludge and whey: enhancement of product properties and potential application in agriculture. *Fuel.* 350, 128807.
- [33] Qi, C., Yin, R., Cheng, J., Xu, Z., Chen, J., Gao, X., Li, G., Nghiem, L., Luo, W., 2022. Bacterial dynamics for gaseous emission and humification during bio-augmented composting of kitchen waste with lime addition for acidity regulation. *Sci. Total Environ.* 848, 157653.
- [34] Rodríguez-Espinosa, T., Papamichael, I., Voukkali, I., Gimeno, A.P., Candel, M.B.A., Navarro-Pedreño, J., Zorpas, A.A., Lucas, I.G., 2023. Nitrogen management in farming systems under the use of agricultural wastes and circular economy. *Sci. Total Environ.* 876, 162666.
- [35] Sarlaki, E., Ghorbani-Isfahani, P., Ghorbani, M., Benedini, L., Kermani, A., Rezaei, M., Marzban, N., Filonenko, S., Peng, W., Tabatabaei, M., He, Y., Aghbashlo, M., Kianmehr, M.H., Angelidaki, I., 2024. Oxidation-alkaline-enhanced abiotic humification valorizes lignin-rich biogas digestate into artificial humic acids. *J. Clean. Prod.* 435, 140409.
- [36] Sarlaki, E., Kianmehr, M.H., Ghorbani, M., Kermani, A.M., Asefpour Vakilian, K., Angelidaki, I., Wang, Y., Gupta, V.K., Pan, J., Tabatabaei, M., Aghbashlo, M., 2023a. Highly humified nitrogen-functionalized lignite activated by urea pretreatment and ozone plasma oxidation. *Chem. Eng. J.* 456, 140978.
- [37] Sarlaki, E., Kianmehr, M.H., Kermani, A., Ghorbani, M., Ghorbani Javid, M., Rezaei, M., Peng, W., Lam, S.S., Tabatabaei, M., Aghbashlo, M., Chen, X., 2023b. Valorizing lignite waste into engineered nitro-humic fertilizer: advancing resource efficiency in the era of a circular economy. *Sustainable Chem. Pharm.* 36, 101283.
- [38] Shan, G., Li, W., Bao, S., Li, Y., Tan, W., 2023. Co-hydrothermal carbonization of agricultural waste and sewage sludge for product quality improvement: fuel properties of hydrochar and fertilizer quality of aqueous phase. *J. Environ. Manage.* 326, 116781.
- [39] Shao, Y., Bao, M., Huo, W., Ye, R., Ajmal, M., Lu, W., 2023a. From biomass to humic acid: Is there an accelerated way to go?. *Chem. Eng. J.* 452, 139172.
- [40] Shao, Y., Bao, M., Huo, W., Ye, R., Liu, Y., Lu, W., 2022. Production of artificial humic acid from biomass residues by a non-catalytic hydrothermal process. *J. Clean. Prod.* 335, 130302.
- [41] Shao, Y., Li, Z., Long, Y., Zhao, J., Huo, W., Luo, Z., Lu, W., 2023b. Direct humification of biowaste with hydrothermal technology: a review. *Sci. Total Environ.* 908, 168232.
- [42] Shrestha, A., Acharya, B., Farooque, A.A., 2021. Study of hydrochar and process water from hydrothermal carbonization of sea lettuce. *Renewable Energy.* 163, 589-598.
- [43] Stevenson, F.J., 1994. *Humus chemistry: genesis, composition, reactions*. John Wiley and Sons.
- [44] Tkachenko, V., Ambrosini, S., Marzban, N., Pandey, A., Vogl, S., Antonietti, M., Filonenko, S., 2024. Fulvic acid modification with phenolic precursors towards controllable solubility performance. *RSC Sustainability.*
- [45] Tkachenko, V., Marzban, N., Vogl, S., Filonenko, S., Antonietti, M., 2023. Chemical insights into the base-tuned hydrothermal treatment of side stream biomasses. *Sustainable Energy Fuels.* 7(3), 769-777.
- [46] Usmani, Z., Sharma, M., Diwan, D., Tripathi, M., Whale, E., Jayakody, L.N., Moreau, B., Thakur, V.K., Tuohy, M., Gupta, V.K., 2022. Valorization of sugar beet pulp to value-added products: a review. *Bioresour. Technol.* 346, 126580.
- [47] VDLUFA, 2012. *Handbuch der landwirtschaftlichen versuchs-und untersuchungsmethodik (vdlufa-methodenbuch), bd. Iii. Die chemische untersuchung von futtermitteln.*
- [48] Wang, R., Li, D., Deng, F., Cao, Z., Zheng, G., 2024. Production of artificial humic acid from rice straw for fertilizer production and soil improvement. *Sci. Total Environ.* 906, 167548.
- [49] Wang, R., Li, D., Zheng, G., Cao, Z., Deng, F., 2023. Co-production of water-soluble humic acid fertilizer and crude cellulose from rice straw via urea assisted artificial humification under room temperature. *Chem. Eng. J.* 455, 140916.
- [50] Wang, X., Shen, Y., Liu, X., Ma, T., Wu, J., Qi, G., 2022. Fly ash and H<sub>2</sub>O<sub>2</sub> assisted hydrothermal carbonization for improving the nitrogen and sulfur removal from sewage sludge. *Chemosphere.* 290, 133209.
- [51] Wang, Y.Y., Jing, X.R., Li, L.L., Liu, W.J., Tong, Z.H., Jiang, H., 2017. Biototoxicity evaluations of three typical biochars using a simulated system of fast pyrolytic biochar extracts on organisms of three kingdoms. *ACS Sustainable Chem. Eng.* 5(1), 481-488.
- [52] Wei, S., Li, Zichen, Sun, Y., Zhang, J., Ge, Y., Li, Zhili, 2022. A comprehensive review on biomass humification: recent advances in pathways, challenges, new applications, and perspectives. *Renew. Sust. Energy Reviews.* 170, 112984.
- [53] Xu, Z., Qi, C., Zhang, L., Ma, Y., Li, G., Nghiem, L.D., Luo, W., 2021. Regulating bacterial dynamics by lime addition to enhance kitchen waste composting. *Bioresour. Technol.* 341, 125749.
- [54] Yang, F., Fu, Q., Antonietti, M., 2023. Anthropogenic, Carbon-Reinforced Soil as a Living Engineered Material. *Chem. Rev.* 123(5), 2420-2435.
- [55] Yang, F., Tang, C., Antonietti, M., 2021. Natural and artificial humic substances to manage minerals, ions, water, and soil microorganisms. *Chem. Soc. Rev.* 50(10), 6221-6239.
- [56] Yang, F., Zhang, S., Cheng, K., Antonietti, M., 2019. A hydrothermal process to turn waste biomass into artificial fulvic and humic acids for soil remediation. *Sci. Total Environ.* 686, 1140-1151.
- [57] Yin, S., Zhang, X., Suo, F., You, X., Yuan, Y., Cheng, Y., Zhang, C., Li, Y., 2022. Effect of biochar and hydrochar from cow manure and reed straw on lettuce growth in an acidified soil. *Chemosphere.* 298, 134191.
- [58] Zhi, Y., Li, X., Lian, F., Wang, C., White, J.C., Wang, Z., Xing, B., 2022. Nanoscale Iron trioxide catalyzes the synthesis of auxins analogs in artificial humic acids to enhance rice growth. *Sci. Total Environ.* 848, 157536.



**Mona Ghaslani** is a Ph.D. student in Civil Engineering and Architecture at the University of Cagliari, Italy. She received her Bachelor's degree in 2020 and her Master's degree in 2023 from the Department of Environmental Health Engineering at the Kurdistan University of Medical Sciences, Sanandaj, Iran. She has been working on the hydrothermal carbonization and humification of agri-food by-products for agricultural and environmental purposes, such as using these

products as soil amendments and studying their effects on plants and *Daphnia*. She will continue to explore this topic in her Ph.D.



**Dr. Reza Rezaee** is Associate Professor of Environmental Health Engineering working in the Department of Environmental Health Engineering, School of Public Health, Kurdistan University of Medical Sciences, Sanandaj, Iran. He graduated with a Ph.D. in Environmental Health Engineering from Tehran University of Medical Sciences, Tehran, Iran, in 2015. He has already supervised more than 10 PhD and Master students. His primary research interests are environmental pollutant

monitoring, water treatment, especially the application of membrane technologies in water treatment and pollutant removal. He has also published over 40 research articles in high quality journals as the main author.



**Dr. Omid Aboubakri** is Assistant Professor of Epidemiology graduated of Epidemiology, PhD from Kerman University of Medical Sciences in 2020. He is now working in Environmental Health Research Center, Kurdistan University of Medical Sciences, Sanandaj, Iran. His main research area is Environmental Epidemiology, especially air quality and health. He is also interested in doing research on the subject using remote sensing data and spatio-temporal models. Dr. Aboubakri has already

published some scientific papers, and currently started a new project on this subject in Iran.



**Ehsan Sarlaki** holds the MSc and PhD in Biosystems Engineering from the University of Tehran, Iran. Ehsan's research interests primarily include organic waste/biomass valorization, characterization, processing, and sustainability and environmental impacts assessment of upcycling technologies (composting, pyrolysis, hydrothermal treatment, carbonization, humification, fulvicification, hydrolysis, formulation, enrichment, extraction, pelletization, drying, etc.). Dr. Sarlaki

serves as a reviewer for several Journals and has published in precious journals like the Journal of Cleaner Production, Bioresource Technology, and Chemical Engineering Journal.



**Thomas Hoffmann** is the head of the Systems Process Engineering department at the Leibniz Institute for Agricultural Engineering and Bioeconomy (ATB), Potsdam, Germany. With a Diploma in Mechanical Engineering, specialized in agricultural machinery, and a Ph.D. in Technology and Plant Production, his expertise spans several critical areas. His leadership covers both scientific and administrative roles across various working groups, including those focused on process engineering for fibre plants, energy crops, thermochemical conversion, drying technology, and the exploration of emerging food resources and technology. His research interests are diverse, covering the harvest, storage, and conservation of agricultural products, development of rheological models, processing of natural fibers, and thermochemical conversion of agricultural residues. Additionally, he has contributed 13 years as a lecturer at Humboldt-University of Berlin, sharing his knowledge on the supply and utilization of biogenic raw materials.



**Afshin Maleki** is currently working as Professor at Department of Environmental Health Engineering, School of Health, Kurdistan University of Medical Sciences, Sanandaj, Iran. He has completed his Ph.D. in Environmental Health Engineering in 2006 from Tehran University of Medical Sciences, Tehran, Iran. He has supervised 40 MSc. and 10 Ph.D. theses and also handled various research projects in Environmental Health Engineering, all of them in Water and Wastewater Engineering

Subjects and Pollution Control. His area of research interest focuses on Environmental Pollution Control and Monitoring, Waste Treatment, material design, AOPs, and Nanotechnology for environmental and health applications. He has published more than 200 research articles in international journals and 50 papers in international conferences contributed as author/co-author.



**Nader Marzban** is currently working as a full-time researcher at the Leibniz Institute for Agricultural Engineering and Bioeconomy (ATB), Potsdam, Germany, with a focus on the thermochemical conversion of biomass, specifically through hydrothermal processes. He completed his PhD in 2023 on hydrothermal carbonization, humification, and fulvicification of agricultural residues under the supervision of Dr. Judy Libra and Prof. Susanne Rotter from the Technical University of Berlin.

During his PhD, he conducted a research stay at the Max Planck Institute of Colloids and Interfaces, department of colloid chemistry, Potsdam, Germany. During his stay, he learned the chemistry behind the hydrothermal carbonization and humification of various biomasses under the supervision of Dr. Svitlana Filonenko and Prof. Markus Antonietti. He has published 18 research papers in peer-reviewed journals. Within the 'Saving a Tree' project, he collaborated with a team to produce and apply artificial humic substances, successfully preserving a 160-year-old beech tree in historical Park Sanssouci, Potsdam, Germany.